



## G0 experiment status

Guillaume Batigne

### ► To cite this version:

Guillaume Batigne. G0 experiment status. ICTP International Conference on Perspectives in Hadronic Physics 4, May 2003, Trieste, Italy. pp.206-211. in2p3-00021888

**HAL Id: in2p3-00021888**

**<https://hal.in2p3.fr/in2p3-00021888>**

Submitted on 14 Jun 2004

**HAL** is a multi-disciplinary open access archive for the deposit and dissemination of scientific research documents, whether they are published or not. The documents may come from teaching and research institutions in France or abroad, or from public or private research centers.

L'archive ouverte pluridisciplinaire **HAL**, est destinée au dépôt et à la diffusion de documents scientifiques de niveau recherche, publiés ou non, émanant des établissements d'enseignement et de recherche français ou étrangers, des laboratoires publics ou privés.

# $G^0$ Experiment Status

G. Batigne for the  $G^0$  Collaboration

Laboratoire de Physique Subatomique et Cosmologie, 38028 Grenoble, France

Received: date / Revised version: date

**Abstract.** The  $G^0$  project is a parity violation experiment dedicated to the measurement of the proton weak and axial form factors by means of elastic electron scattering. Combining these weak form factors with the known electromagnetic ones makes possible the extraction of the contribution of strange quarks to the charge and magnetization distributions in the nucleon. After introducing the physics case, this paper describes the  $G^0$  apparatus and the measurements planned. An engineering run of this experiment took place recently ; first results are presented.

**PACS.** PACS-key describing text of that key – PACS-key describing text of that key

## 1 Introduction

The nucleon is naively viewed as a set of three valence quarks (uud for the proton and udd for the neutron) but its internal structure is far more complicated. In Quantum Chromodynamics (QCD), the quarks are bound by the strong interaction mediated by the exchange of gluons which can fluctuate into quark-antiquark pairs ( $u\bar{u}$ ,  $d\bar{d}$ ,  $s\bar{s}$ , ...). Thus the nucleon is a set of valence quarks surrounded by a “sea” of gluons and quark-antiquark pairs. At low energy, the strong interaction cannot be treated by the theory of perturbative QCD which implies that the structure of the nucleon cannot be easily described. Experiments are then required to constrain theoretical models and to gain a better understanding of the structure of hadrons.

Some experimental results have already given indications that the strange quarks contribute to the properties of the nucleon. The  $\sigma$ -term value in  $\pi N$  scattering suggests a contribution of strange quarks of about 130 MeV to the nucleon mass [1]. From  $eN$  Deep Inelastic Scattering data, strange quarks could contribute to the nucleon spin at the level of few percent ( $\langle N | \bar{s} \gamma^\mu \gamma^5 s | N \rangle \simeq -10\%$  [2]). But those results are still questionable due to theoretical assumptions or unmeasured contributions.

The purpose of Parity Violating (PV) experiments in electron scattering is to extract the contribution of strange quarks to the charge and magnetization distributions of the nucleon. The formalism and the principle of these measurements are first presented. Then the  $G^0$  experiment is described and first results from its engineering run are given.

## 2 Strangeness and Parity Violation

The extended structure of nucleons has been extensively studied by electron scattering. The virtual photon, exchanged during the reaction, probes the internal electromagnetic structure of the nucleons. The elastic cross section ( $eN$ ) depends on Dirac and Pauli form factors,  $F_1^\gamma$  and  $F_2^\gamma$  respectively, which describe the electromagnetic structure of nucleons. These form factors depend only on the four-momentum carried by the virtual photon ( $Q^2$ ). By varying the value of  $Q^2$ , one can tune the probed spatial dimension. One can also use the Sachs form factors, defined as follows :

$$G_E^\gamma = F_1^\gamma - \tau F_2^\gamma \quad G_M^\gamma = F_1^\gamma + F_2^\gamma \quad (1)$$

where  $\tau = Q^2/(4M_N^2)$  with  $M_N$  the mass of the nucleon. In the Breit frame,  $G_E^\gamma$  and  $G_M^\gamma$  are respectively the Fourier Transforms of the spatial distributions of the charge and magnetization in the nucleon [3]. These form factors are related to the static properties of the nucleon (at  $Q^2 = 0$ ) :

$$G_E^{\gamma,N}(0) = Q_N \quad G_M^{\gamma,N}(0) = \mu_N \quad (2)$$

where  $Q_N$  is the charge and  $\mu_N$  the magnetic moment of the nucleon  $N$ . Another quantity of interest is the charge radius which is defined as follows :

$$\langle r^2 \rangle = -6 \left. \frac{dG_E}{dQ^2} \right|_{Q^2=0} \quad (3)$$

As photons couple only to quarks in the nucleon, the form factors can be expressed as the sum of the contributions from the different quark flavors,  $G_{E,M}^{q,N}$ . The sea quarks are produced from the fluctuations of gluons in quark-antiquark pairs. The probability of this process is proportional to  $1/M_q^2$  where  $q$  is the flavor of the produced

quarks. At the energy of the current experiments, one can neglect the contribution of the heaviest quarks ( $c$ ,  $b$  and  $t$ ) and express the electromagnetic Sachs form factors as follows :

$$G_{E,M}^{(\gamma,N)} = \sum_{q=u,d,s} e_q G_{E,M}^{q,N} \quad (4)$$

The values of the electromagnetic form factors  $G_{E,M}^{(\gamma,p)}$  and  $G_{E,M}^{(\gamma,n)}$  have been or are presently measured for  $Q^2$  values up to 1  $(\text{GeV}/c)^2$ . These form factors provide four relations but there are twelve unknowns ( $G_{E,M}^{q,N}$ ). To reduce this number to six, the hypothesis of isospin symmetry is made :  $G_{E,M}^{u,p} = G_{E,M}^{d,n} = G_{E,M}^u$ ,  $G_{E,M}^{d,p} = G_{E,M}^{u,n} = G_{E,M}^d$  and  $G_{E,M}^{s,p} = G_{E,M}^{s,n} = G_{E,M}^s$ . The measurement of the contribution of the strange quarks ( $G_{E,M}^s$ ) requires then two additional independent combinations of  $G_{E,M}^{q,N}$  to solve the system.

Similarly to the electromagnetic interaction, one can also define Sachs form factors for the weak interaction,  $G_{E,M}^{(Z,N)}$  ( $Z$  boson exchange in  $eN$  scattering). As the  $Z$  boson also couples only to quarks in the nucleon, the weak form factors of the proton can be written as :

$$G_{E,M}^{(Z,p)} = \sum_{q=u,d,s} C_V^q G_{E,M}^{q,p} \quad (5)$$

where  $C_V^q = 2T_3 - 4Q_q \sin^2 \theta_W$  is the weak vector charge of quarks of flavor  $q$  [5]. As the weak interaction violates parity symmetry, there is also an axial form factor  $G_A^e$ . The two weak form factors of the proton represent then two new independent combinations. The strange contributions to charge and magnetization can then be extracted using the following formula [4] :

$$G_{E,M}^s = (1 - 4 \sin^2 \theta_W) G_{E,M}^{(\gamma,p)} - G_{E,M}^{(\gamma,n)} - G_{E,M}^{(Z,p)} \quad (6)$$

Thus the determination of strange quark contributions requires the measurement of weak form factors of the proton, as, contrary to electromagnetic form factors, these weak form factors are still mostly unknown.

The elastic scattering ( $eN$ ) cross section depends in fact on both electromagnetic and weak form factors. But for values of  $Q^2$  around 1  $(\text{GeV}/c)^2$ , the weak element matrix,  $M_Z$ , is  $10^{-5}$  smaller than the electromagnetic one associated to the exchange of a virtual photon,  $M_\gamma$ . The experimental systematic errors related to normalization prevent then the weak form factors to be obtained from unpolarized cross section measurements. Contrary to the electromagnetic interaction, the parity symmetry is violated in the weak interaction. Consequently the cross section of elastic scattering of longitudinally polarized electrons on nucleons ( $\vec{e}N$ ) depends on the helicity of the incident electrons (i.e.  $\sigma_+ \neq \sigma_-$ , where  $\pm$  refers to the two possible helicity states). Thus the weak part of the scattering can be extracted by a parity violation asymmetry measurement :

$$A_{PV} = \frac{\sigma_+ - \sigma_-}{\sigma_+ + \sigma_-} \quad (7)$$

**Table 1.** Values in part per million (ppm) of  $A_{s=0}$ ,  $\eta$ ,  $\chi$  and  $\xi$  for the kinematical condition of the  $G^0$  experiment and for  $Q^2=0.5$   $(\text{GeV}/c)^2$ .

	$\theta_e$	$A_{s=0}$ (ppm)	$\eta$ (ppm)	$\chi$ (ppm)	$\xi$ (ppm)
$A_F$	$13^\circ$	-16.7	<u>60.8</u>	25.0	1.4
$A_B$	$110^\circ$	-29	18.0	<u>40.3</u>	8.5
$A_D$	$110^\circ$	-39.8	14.7	9.0	<u>10.1</u>

Because of the smallness of the weak interaction, the asymmetry is of the order of  $10^{-5}$  but this time many normalization terms (i.e. luminosity, acceptance, ...) cancel in the ratio. This parity violation asymmetry is a function of electromagnetic, weak and axial form factors [5,6] :

$$A_{PV}(Q^2, \theta_e) = -\frac{G_F Q^2}{4\sqrt{2}\pi\alpha} \frac{f_E G_E^{(Z,N)} + f_M G_M^{(Z,N)} + f_A G_A^e}{A_D} \quad (8)$$

where

$$\begin{aligned} f_E &= \epsilon G_E^{(\gamma,p)}, \quad f_E = \tau G_M^{(\gamma,p)}, \quad f_A = \epsilon' G_M^{(\gamma,p)} \\ A_D &= \epsilon \left( G_E^{(\gamma,p)} \right)^2 + \tau \left( G_M^{(\gamma,p)} \right)^2 \end{aligned} \quad (9)$$

The kinematical factors  $\epsilon$ ,  $\tau$  and  $\epsilon'$  are function of  $Q^2$  and  $\theta_e$ , the electron scattering angle in the laboratory frame. Formula 8 can also be expressed as a function of  $G_E^s$ ,  $G_M^s$  and  $G_A^e$  :

$$A_{PV} = A_{s=0} + \eta G_E^s + \chi G_M^s + \xi G_A^e \quad (10)$$

where  $A_{s=0}$ , the value of the asymmetry with no strange quarks contribution, is derived from the Standard Model predictions and the measured electromagnetic form factors. The terms  $\eta$ ,  $\chi$  and  $\xi$  depend on kinematics of the electron scattering and electromagnetic form factors. Formula 10 shows that the asymmetry is sensitive to a linear combination of  $G_E^s$ ,  $G_M^s$  and  $G_A^e$ . Thus for a given value of  $Q^2$ , a set of three measurements must be performed to separate them. The first two measurements correspond to electron scattering on proton in the forward ( $A_F$ ) and backward ( $A_B$ ) directions. The axial form factor,  $G_A^e$ , can be calculated from theoretical predictions. However due to difficulties of estimating its value and  $Q^2$  dependence, it appears worth also measuring it. Thus a third measurement ( $A_D$ ) is performed on deuterons at backward angles in quasi-elastic scattering. The different values of  $A_{s=0}$ ,  $\eta$ ,  $\chi$  and  $\xi$  are reported in table 1 for  $Q^2=0.5$   $(\text{GeV}/c)^2$  and for the electron scattering angles used in the  $G^0$  experiment. From the values quoted in this table, one can see that the measurement at forward angle ( $A_F$ ) is the most sensitive to  $G_E^s$ . The backward angle measurement on protons ( $A_B$ ) is more sensitive to  $G_M^s$  and a measurement on deuterons ( $A_D$ ) gives a way to extract the axial form factor.

Two parity violation experiments have already published results. The first one, SAMPLE at MIT-Bates, measured

backward angle scattering ( $130^\circ < \theta_e < 170^\circ$ ) asymmetries on  $LH_2$  at  $Q^2 = 0.1$  (GeV/c) $^2$  [7]. A second measurement was performed at the same kinematics but on deuterium [8]. The combination of the two results gives the following values for  $G_M^s$  and the isovector part of  $G_A^e$  :

$$G_M^s = 0.14 \pm 0.29 \pm 0.31 \quad (11)$$

$$G_A^e(T=1) = 0.22 \pm 0.45 \pm 0.39 \quad (12)$$

where the first error corresponds to statistics and the second to systematics (errors on beam properties, electromagnetic form factors, etc.). The second experiment, HAPPEX at Jefferson Laboratory, measured the asymmetry on  $LH_2$  at  $Q^2=0.48$  (GeV/c) $^2$  and forward scattering angle ( $\theta_e = 12.5^\circ$ ) [9,10]. This experiment extracted a linear combination of  $G_E^s$  and  $G_M^s$  :

$$G_E^s + 0.392G_M^s = 0.025 \pm 0.020 \pm 0.014 \quad (13)$$

The effect of strange quarks is small but the individual electric and magnetization contributions of strange quarks cannot be separated in a single measurement ; also a limited range of  $Q^2$  is presently covered. An experimental effort is thus still underway. The PVA4 experiment [11] at Mainz will separate  $G_E^s$  and  $G_M^s$  at  $Q^2=0.225$  (GeV/c) $^2$ . The HAPPEX2 experiment on the proton and on  $^4\text{He}$ , at JLab, will be able to make the separation of  $G_E^s$  and  $G_M^s$  at the same  $Q^2$  as the SAMPLE experiment.

This contribution details the  $G^0$  experiment which is now starting to take data. The aim of this project is to separate  $G_E^s$ ,  $G_M^s$  and  $G_A^e$  for three values of  $Q^2$  : 0.3, 0.5 and 0.8 (GeV/c) $^2$  [12]. The expected precision on  $G_E^s$ ,  $G_M^s$  and  $G_A^e$  and the wide range of  $Q^2$  covered by this experiment can be seen in figure 1 to be quite unique.

Theoretical models have been used to predict the contributions of strange quarks [13]. Models are based on chiral perturbation theory [14], Vector Dominance Meson approaches [15] and lattice QCD techniques [16] and provide values of  $G_E^s$  and  $G_M^s$ . Some of these predictions are reported in figure 1, compared with projected experimental results. One can see that the models give different strange quark contributions. So experimental results are required to constrain these theoretical models. About the isovector axial form factor, its value at  $Q^2 = 0$  (GeV/c) $^2$  was calculated by Zhu *et al* [17] and its  $Q^2$  dependence by Maekawa *et al* [18]. Their results were combined and are reported in figure 1. The only published experimental result is given by the SAMPLE collaboration and has a large error. In these figures are also reported expected errors for HAPPEX2 and  $G^0$  experiments. So this set of new experiments will strongly constrain theoretical models.

### 3 $G^0$ Experiment

The values of asymmetries to be measured by parity violation experiments are of the order of  $10^{-5}$ . However one requires an absolute precision of  $10^{-6} - 10^{-7}$ , and thus all false asymmetry sources must be controlled to high precision. There are thus general requirements that must

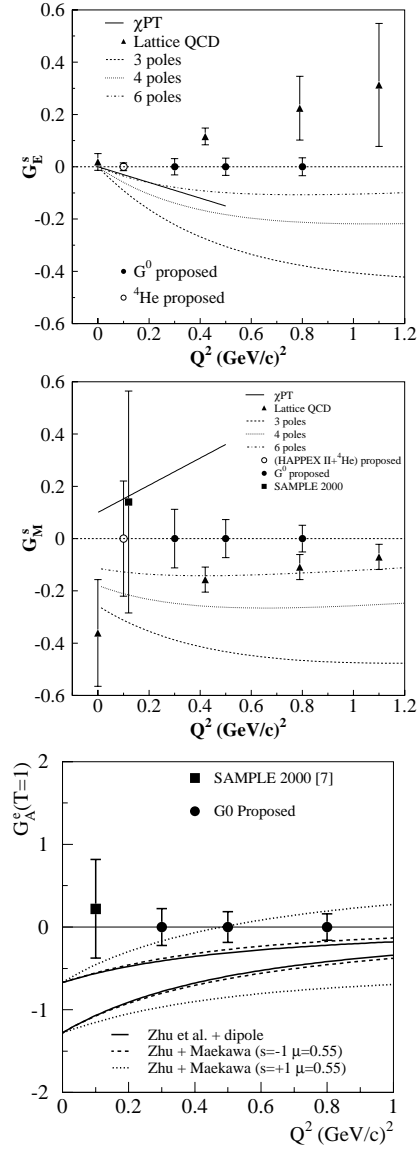


**Fig. 1.** Predictions of some theoretical models on  $G_E^s$ ,  $G_M^s$  and  $G_A^e(T=1)$ . The expected errors of approved experiment at JLab and the results of SAMPLE are also shown (figures taken from [19], references therein).

be fulfilled for a violation parity experiment. This is in particular the case for the beam properties. First the polarization has to be known at the few percent level because the measured asymmetry is proportional to the beam polarization. The helicity reversal must happen with a high frequency (30-60 Hz typically) to minimize the effects of slow drift, especially on intensity. Feedback systems on intensity, energy and position are used to keep the beam properties as close as possible in the two helicity states and thus to limit corrections to be applied in the asymmetry calculation. To achieve a statistical precision of  $10^{-7}$ , one has to record  $10^{14}$  events, requiring a large luminosity. The parity violation experiments use long (between 20 and 40 cm) cryogenic targets and high beam intensity. A

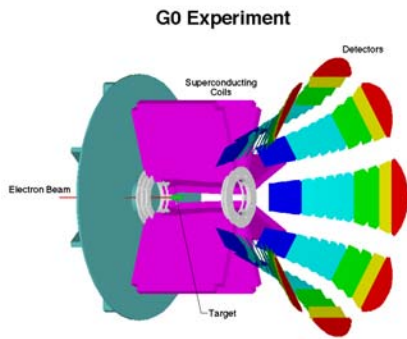


Fig. 2. The  $G^0$  apparatus.

full data acquisition event by event is also excluded. The measurement is therefore made by the integration of a signal or summing events in histograms. Also fast detectors (typically 10 ns) are used. The dead time of electronics and acquisition must be as low as possible.

The  $G^0$  experiment that is being described in this contribution is a parity violation experiment which is taking place at Jefferson Laboratory (JLab, Virginia, USA). The collaboration is formed of North-American, Armenian and French institutes and universities [12]. This experiment is installed in Hall C of JLab. The CEBAF accelerator delivers us electron beam with 75% polarization and 40  $\mu$ A intensity. This beam is pulsed with a period of 32 ns.

In order to separate the weak form factors, the  $G^0$  experiment is scheduled into two distinct sets of measurements. The first phase is dedicated to the measurement at forward scattering angles ( $A_F$ ) and the final data taking will take place early 2004. It will measure the parity violation asymmetry for  $Q^2$  values ranging between 0.1 and 1 (GeV/c)<sup>2</sup> using a single beam energy (3 GeV). The  $G^0$  set-up is first composed of a 20 cm long target which can be filled with liquid hydrogen or deuterium. This target is located at the center of a toroidal superconducting magnet. The produced field bends charged particles on a focal plane where are located a set of detectors (FPD<sup>1</sup>) formed of scintillator pairs, optically coupled to phototubes. Eight sectors of detection (octants) are used, each formed of 16 FPD detectors. The set-up is shown in figure 2. The shape and position of each detector are designed in such a way that it covers a given range in  $Q^2$ . The scattering angle of electrons is varying between 6° and 22°. As the detection of electrons is very difficult at these angles, the recoil protons instead are detected ( $48^\circ < \theta_p < 78^\circ$ ). The background formed by neutrals ( $\gamma$  and neutrons) is mostly removed by a set of internal collimators preventing direct view of the target. The background formed by charged particles ( $\pi^+$  and inelastically scattered protons) is rejected by a Time of Flight (ToF) measurement. For each FPD detector, a ToF spectrum is constructed. Figure 3 shows an example of a simulated ToF spectrum. The beam time structure is chosen so that all particles produced by a beam burst ev-

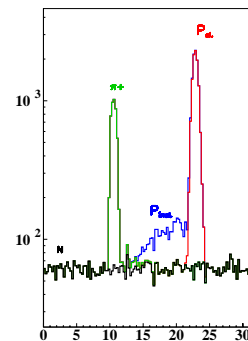


Fig. 3. Example of a simulated ToF spectrum. The vertical axis represents relative counting rates and the horizontal axis ToF is expressed in ns.

ery 32 ns are detected before the arrival of the next beam burst. The elastically scattered protons can be selected by cuts on ToF. Custom electronics were designed and allow to discriminate photomultiplier signals, make the coincidence between the two layers of scintillator for each detector<sup>2</sup> and generate the ToF spectra. These histograms are read during each helicity reversal which occurs at a frequency of 30 Hz. This procedure eliminates deadtime related to the data acquisition.

The second phase of the  $G^0$  experimental program will be dedicated to back angle measurements (both on  $LH_2$  and  $LD_2$ ) and should take place in 2005-2006. In contrast with the first phase, electrons are detected. Their scattering angle is around 110° and the value of  $Q^2$  varies slowly in the acceptance of the collimators. Therefore the measurements will be performed at three beam energies (420, 580 and 800 MeV) and values of  $Q^2$  equal to 0.3, 0.5 and 0.8 (GeV/c)<sup>2</sup> will be accessible. To detect particles scattered at backward angles, the overall apparatus must be turned around. The detected electrons are ultra-relativistic so a ToF measurement cannot be used to reject the background<sup>3</sup>. Thanks to the magnetic field of the spectrometer, elastically scattered electrons have different trajectories compared to inelastically scattered electrons and  $\pi^-$ . So eight hodoscopes composed of nine additional scintillator detectors, called CEDs<sup>4</sup>, will be installed at the exit of the magnet cryostat and associated to each octant of FPD. A coincidence matrix between CED and FPD detectors allows one to separate elastic and inelastic events as shown in figure 4. The asymmetry will be calculated from the counting rates corresponding to the matrix locations associated to elastically scattered electrons. Pions are however also detected in some of the matrix locations associated to elastically scattered electrons. To discriminate and reject these pions, which rates would become very high with a deuterium target, an aerogel

<sup>1</sup> Focal Plan Detector

<sup>2</sup> This allows additional rejection of neutrals.

<sup>3</sup> In this part of the experiment the charged background is  $\pi^-$  and inelastically scattered electrons.

<sup>4</sup> Cryostat Exit Detectors

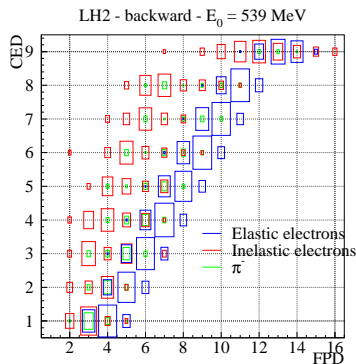


**Fig. 4.** Typical simulated coincidence matrix between CED and FPD detectors.

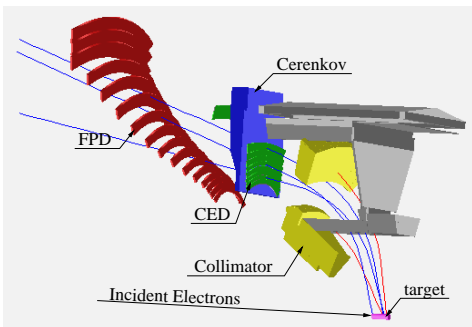


**Fig. 5.** Sketch of one octant of detectors in the back angle configuration. The collimators are used to select the kinematical range but also to shield detectors from the line of sight of the target.

Čerenkov detector will be installed close to the CED hodoscope (see figure 5). The refractive index of the aerogel is chosen so that only electrons produce light when passing through the Čerenkov detector. The Čerenkov signal is consequently used to validate the encoding of an event. This procedure allows the rejection of typically 95% of the pions. The Čerenkov detectors are under construction and test. New custom electronics is presently designed and will form the coincidence matrix and process the Čerenkov signal.

## 4 Engineering run

The first engineering run of the  $G^0$  experiment took place from October 2002 to January 2003 in the forward angle configuration ( $A_F$ ). During this period, not only the apparatus was tested but also many special features required of the CEBAF beam. First the accelerator succeeded to deliver the  $G^0$  beam with use of a new laser system. The standard CEBAF beam is pulsed with a 2 ns period with an intensity up to 100  $\mu$ A. The challenge was to build a 40  $\mu$ A beam with a 32 ns period which means to have 6 times more electrons than usual per burst. Various feed-back systems were also tested. The goal is to achieve, for

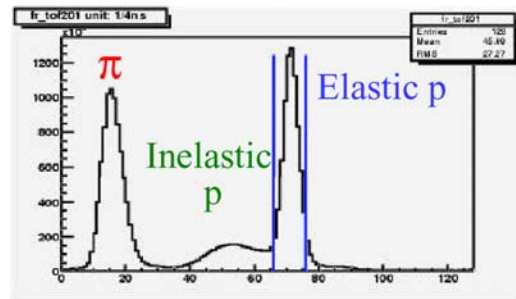


**Fig. 6.** Example of a measured ToF spectrum. The time binning is 0.250 ns.

the 700 h of data taking scheduled for the production run, an overall charge asymmetry less than  $\Delta I/I < 1$  ppm and differences in position less than  $\Delta X < 20$  nm. The amount of useful data for asymmetry calculation recorded during this engineering run represents only 1/16 of the final statistics. For these data, the charge asymmetry was less than 5 ppm and the position asymmetries less than 50 nm which meet the requirements for these recorded data. The target system was also tested ; in particular we checked that it can stand the beam intensity without boiling. A key point for the experiment concerned the operation of the spectrometer. The nominal value of current was achieved in its superconducting mode. The magnetic field is directly related to the  $Q^2$  range measured by the experiment ( $0.1 < Q^2 < 1$  (GeV/c) $^2$ ). The first part of this engineering revealed that the hall background was higher than expected. It was found that the main source of background were neutrals generated at the beam pipe. So the shielding was properly improved. Concerning the detectors, the high voltages for photomultipliers (PMT) were set at values allowing high detection efficiency and the PMTs were able to stand rates at nominal beam current. The gains were matched and their stability was satisfactory over time and different beam conditions. Discriminator thresholds were adjusted in order to remove the noise and low energy particle background while keeping 100% efficiency for elastic proton detection. All electronic channels worked fine and ToF spectra were found stable in time. An example of ToF spectrum is given in figure 6 (the vertical lines in this figure represent typical ToF cuts to select elastic protons). Some studies are still in progress, in particular regarding the deadtime corrections.

The results of the engineering run also show that the rates of inelastic events were higher than expected from the simulations. The main source of these additional events was assigned to reactions occurring in the aluminium target cell windows. So the thickness of these windows will be reduced for the next engineering run scheduled this fall. A check of agreement between simulation, and the understanding of the set-up, and measurement has been made using the ToF difference between pions and elastic protons. Figure 7 shows the results of this study for each detector. The observed agreement is quite good (around 100 ps) and required the inclusion of detailed geometry and event generators in the simulation. This ToF differ-

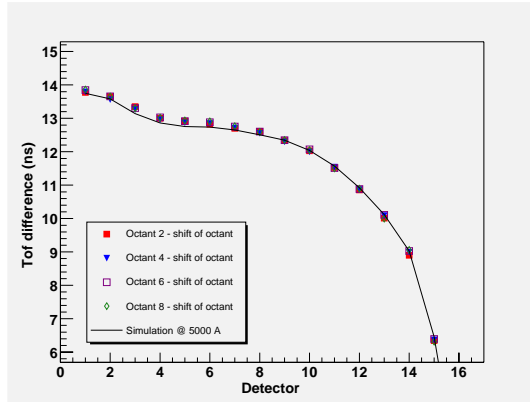


**Fig. 7.** Comparison of the ToF difference between elastic proton and  $\pi^+$  extracted from the simulation (black line) and measurement (points).

ence is also important as it allows to determine the mean value of  $Q^2$  associated with each FPD detector. Indeed pions are ultrarelativistic with almost fixed ToF contrary to protons for which the kinetic energy is proportional to  $Q^2$ . In order to keep the systematic error introduced by the uncertainty on  $Q^2$  below 5% of the statistical error, the value of  $Q^2$  must be known with a precision of 1%. This is achieved with the observed precision of 100 ps on  $\Delta ToF$ .

The parity violation asymmetries have been calculated for each detector. The statistical error associated with this engineering run is about four times larger than the one expected in production run. A Half Wave Plate (IHWP) can be inserted at the injector to reverse the electron helicity compared to the helicity signal sent to the electronics. If there is no false asymmetry generated from the beam or the electronics the results with and without this IHWP must be exactly the same but with opposite sign. Figure 8 shows that it is the case within errors (only statistical ones are displayed). The analysis is still underway. The asymmetry of inelastic events has to be subtracted from the measured asymmetry in order to extract the elastic proton asymmetry. Another study performed at present is related to the electronics response to the charge asymmetry. The goal is to achieve a systematic error at the order of 1% of the charge asymmetry. The main contribution to this systematic error is the deadtime which is proportional to the counting rates. The understanding of the beam properties and feedback systems is also in progress. Improvements and changes will be tested during the next engineering run this fall.

## 5 Conclusions

The purpose of parity violation measurements in ( $eN$ ) elastic scattering is to determine the contribution of strange quarks to the charge and magnetization distributions of the nucleon. Several experimental programs are dedicated to these measurements : SAMPLE at MIT-

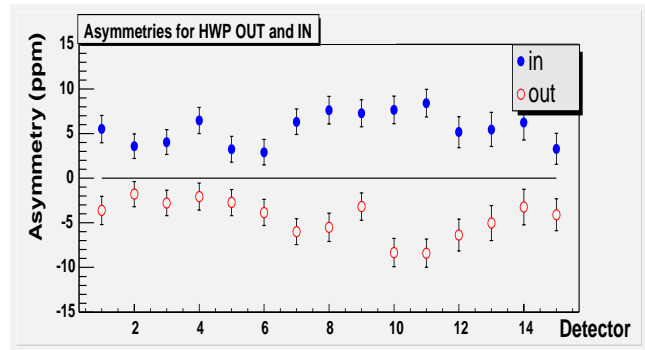


**Fig. 8.** Comparison of the measured asymmetries with and without the Insertable Half Wave Plate (IHWP).

Bates, HAPPEX at JLab, PVA4 at Mainz and  $G^0$  at JLab. The special contribution of the  $G^0$  experiment is that it will be the first experiment to extract  $G_E^s$ ,  $G_M^s$  and  $G_A^e$  over a large range of  $Q^2$  ( $= 0.3, 0.5$  and  $0.8$  (GeV/c) $^2$ ). The results from the first engineering run demonstrate a good understanding of the beam properties, detector and electronics responses. The physics analysis is under way and the data taking production run will take place at the beginning of the next year.

## References

1. J. Glaser, H. Leutwyler and M. Saino, Phys. Lett. **B253**, (1991) 252
2. K. Abe *et al.*, Phys. Rev. **D58**, (1998) 112003
3. F. J. Ernst, R. G. Sachs and K. C. Wali, Phys. Rev. **119** (1960) 1105
4. D.H. Beck and R.D. McKeown, Ann. Rev. Nucl. **51** (2001) 189
5. M. Musolf *et al.*, Phys. Rep. **239**, (1994) 1
6. P.A. Souder and K.S. Kumar, Prog. Part. Nucl. Phys. **45**, (2000) S333
7. R. Hasty *et al.*, Science **290**, (2000) 2117
8. D. Spayde *et al.*, Phys. Rev. Lett. **84**, (2000) 1106
9. K.A. Aniol *et al.*, Phys. Rev. Lett. **82**, (1999) 1096
10. K.A. Aniol *et al.*, Phys. Lett. B **509**, (2001) 211
11. F.E. Maas *et al.* (PVA4 Collaboration), Eur. Phys. J. A **17**, 339 (2003)
12.  $G^0$  web page : <http://www.npl.uiuc.edu/exp/G0/G0Main.html>
13. D.H. Beck and B.R. Holstein, Int. Jour. Mod. Phys. E **10**, (2001) 1
14. T.R. Hemmert, B. Kubis and U.-G. Meißner, Phys. Rev. C **60**, (1999) 045501
15. H. Forkel, Phys. Rev. C **56**, (1996) 510
16. S.J. Dong, K.F. Liu and A.G. Williams, Phys. Rev. D **58**, (1998) 074504
17. S. Zhu *et al.*, Phys. Rev. D **62**, (2000) 033008
18. C.M. Maekawa, J.S. Veiga and U. Van Kolck, Phys. Lett. B **488**, (2000) 167
19. R. Tieulent, PhD Thesis, Grenoble University, ISN 02-27